Supporting Information for:

Nanosized Chevrel Phases for Dendrite-Free Zinc-Ion Based Energy Storage: Unraveling the Phase Transformations

Amr Elgendy[a,b,c], Athanasios A. Papaderakis[a,b], Andinet Ejigu[a,b], Katharina Helmbrecht[d,e], Ben F. Spencer[f], Axel Groß[d,e], Alex S. Walton[a,f], David J. Lewis[g]*, Robert A. W. Dryfe[a,b]*

[a]Department of Chemistry, University of Manchester, Oxford Road, Manchester, M13 9PL, United Kingdom

[b] Henry Royce Institute, University of Manchester, Oxford Road, Manchester, M13 9PL, United Kingdom

[c] Egyptian Petroleum Research Institute, 11727, Cairo, Egypt.

[d] Institute of Theoretical Chemistry, Ulm University, Albert-Einstein-Allee 11, 89081 Ulm, Germany

[e] Helmholtz Institute Ulm (HIU) for Electrochemical Energy Storage, Helmholtzstraße 11, 89081 Ulm, Germany

[f] Photon Science Institute, University of Manchester, Oxford Road, Manchester, M13 9PL, United Kingdom

[g] Department of Materials, University of Manchester, Oxford Road, Manchester, M13 9PL, United Kingdom

Corresponding Authors

*E-mail: david.lewis-4@manchester.ac.uk Tel: +44 (0) 161-306-3561. (D.J.L.)

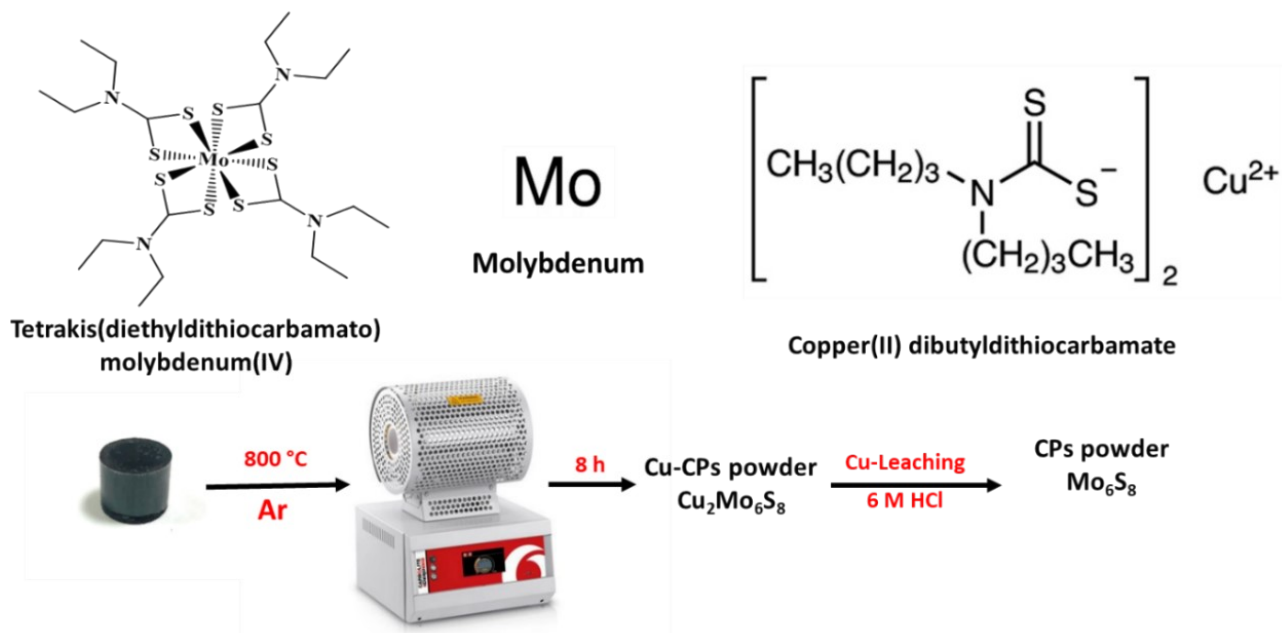 *E-mail: robert.dryfe@manchester.ac.uk Tel: +44 (0) 161-306-4522. (R.A.W.D).

Tetrakis(diethyldithiocarbamato)
molybdenum(IV)

Mo

Molybdenum

Copper(II) dibutyldithiocarbamate

800 °C

Ar

8 h

Cu-CPs powder
$Cu_2Mo_6S_8$

Cu-Leaching

6 M HCl

CPs powder
Mo_6S_8

Figure S1. Schematic illustration of the Mo_6S_8 nanocubes preparation process.

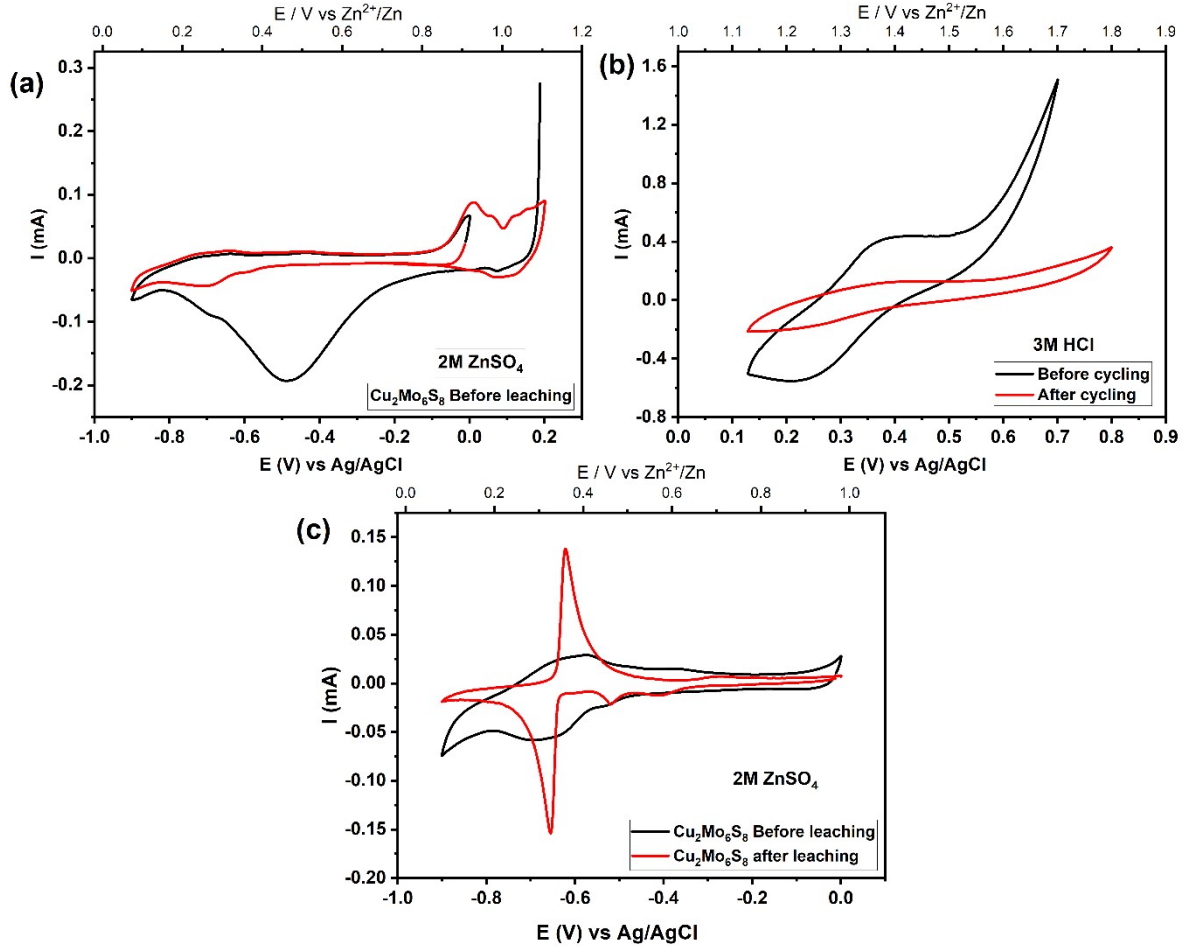**Figure S2.** Characterisation of the electrochemical leaching of Cu: (a) CV of non-leached Cu-Mo_6S_8 in 2M $ZnSO_4$ electrolyte at 5 mV/s. (b) CV of non-leached $CuMo_6S_8$ before and after cycling in 3M HCl at 200 mV/s for 100 cycles. (c) CV of non-leached $Cu_2Mo_6S_8$ and leached Mo_6S_8 in 2M $ZnSO_4$ electrolyte at 5 mV/s.

Generally, Cu in the as-prepared $Cu_2Mo_6S_8$ can be removed through chemical leaching.[1,2] This process involves immersing the $Cu_2Mo_6S_8$ powder in a solution of 6 M HCl (Fisher Scientific, Inc.) and stirring for 10 hours while bubbling oxygen through the solution. However, this process can also be achieved electrochemically by cycling the $Cu_2Mo_6S_8$ in 3 M HCl. Fig.S1a shows the cyclic voltammetry (CV) of the non-leached $Cu_2Mo_6S_8$ in 2 M $ZnSO_4$ electrolyte at a scan rate of 5 mV/s. The absence of redox peaks indicates the presence of Cu ions as the zinc ions are not able to intercalate into Mo_6S_8. Following the electrochemical leaching process of the as-prepared material in 3 M HCl (Fig.S1b), the redox peaks associated with the interaction of Zn and Mo_6S_8 can be observed upon cycling the electrode in 2 M $ZnSO_4$ electrolyte, demonstrating the successful leaching of Cu ions using the electrochemical process.
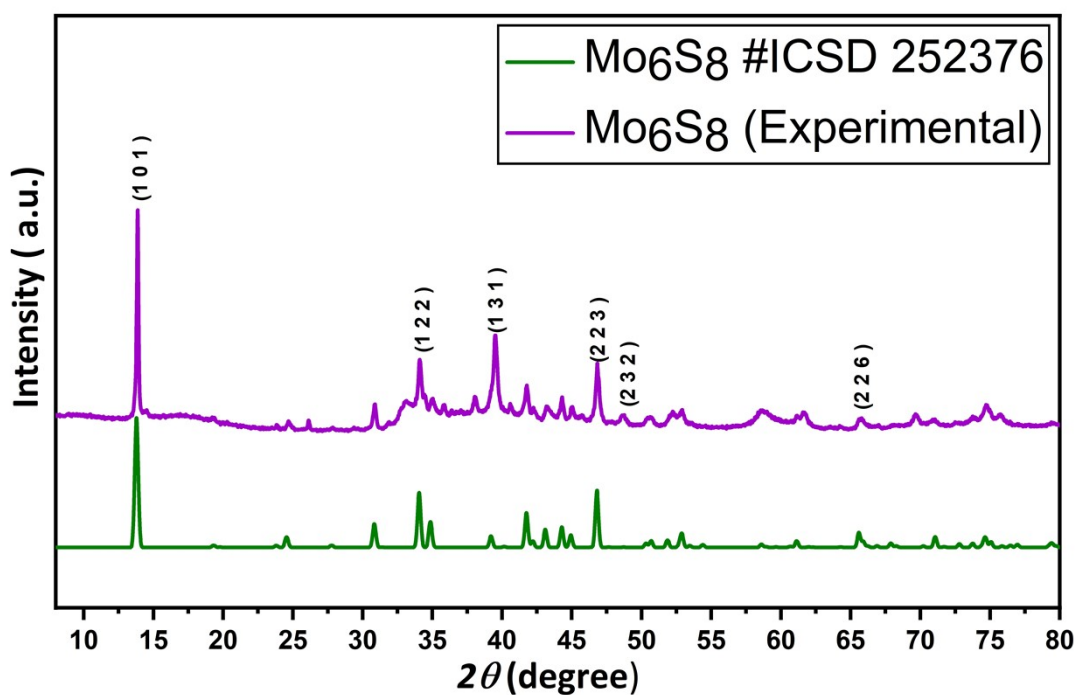
Figure S3. P-XRD characterisation of the prepared Mo_6S_8 along with the corresponding standard pattern.
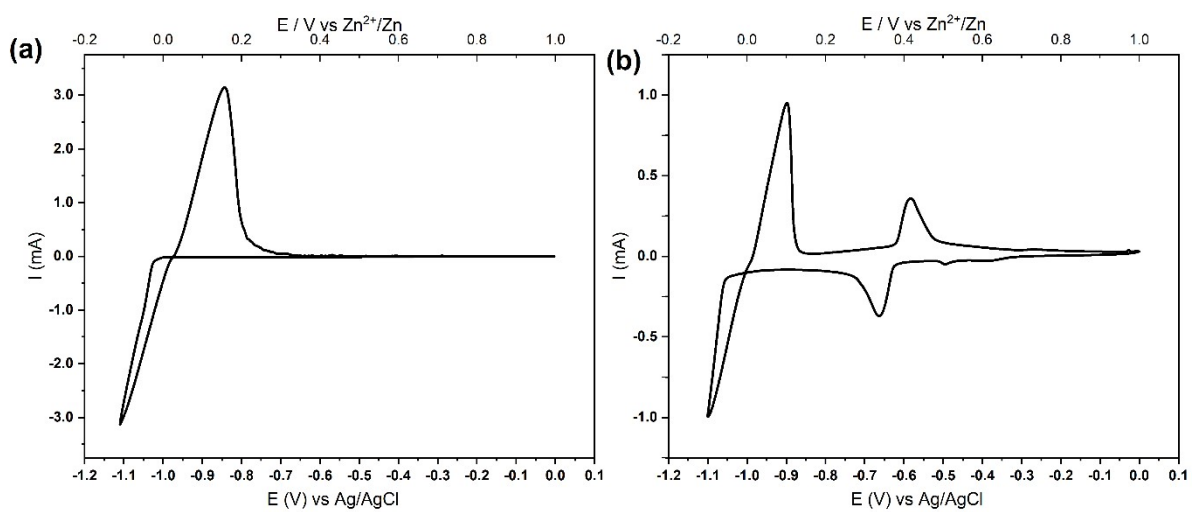

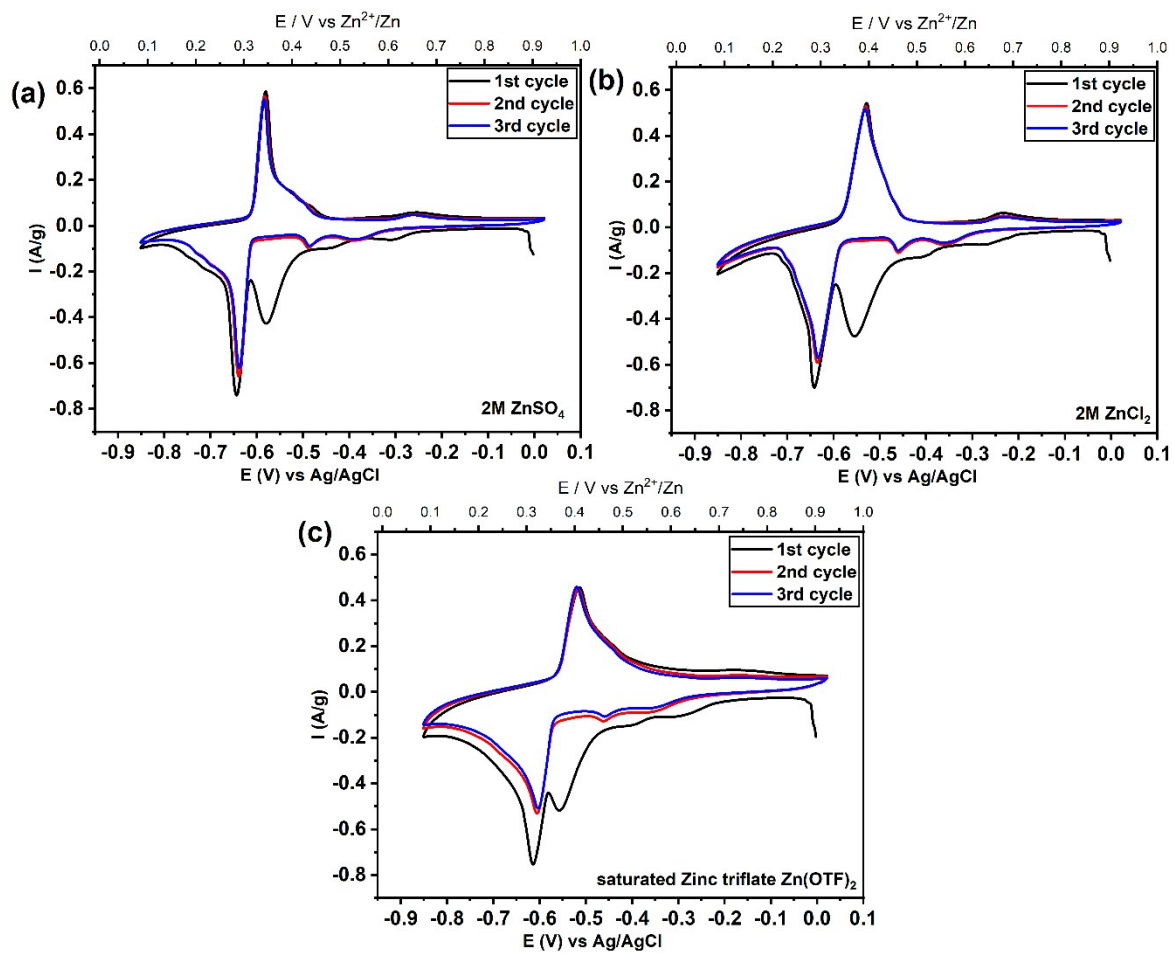**Figure S4.** CVs of bare GC (a) and GC-modified Chevrel phase electrodes in 2 M $ZnSO_4$ at a scan rate of 3mV/s.

Figure S5. Electrochemical CV plots of Chevrel phase at 3mV/s in different zinc electrolytes **(a)** 2M ZnSO4, (b) 2M ZnCl$_2$, and (c) saturated Zn(OTF)$_2$ electrolyte.
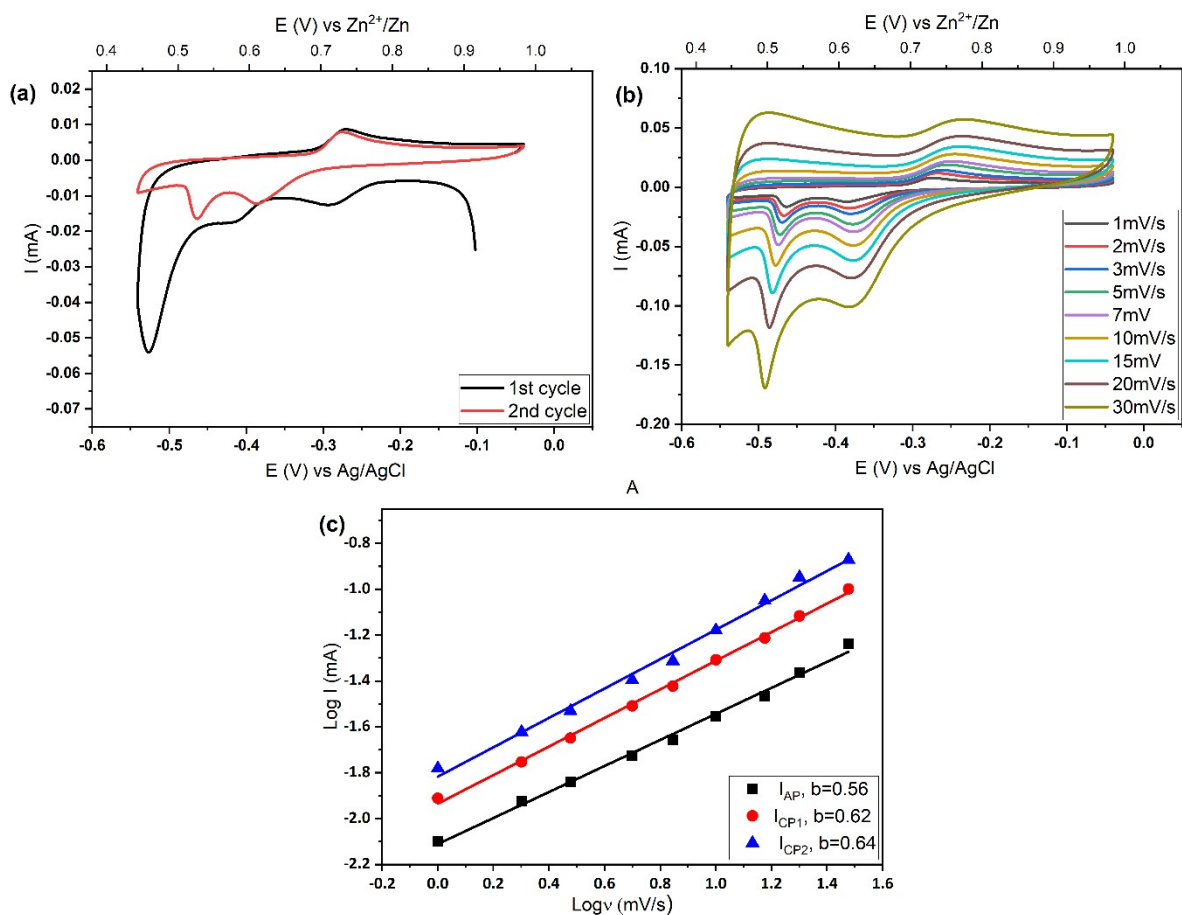
Figure S6. Electrochemical performance of Mo_6S_8 in 2M $ZnSO_4$. (a) CVs of Mo_6S_8 at a scan rate of 1 mV/s in the potential range of −0.01 to −0.55 V vs Ag/AgCl. (b) CV plots at different scan rates from 1 to 30 mV/s. (c) The log (I) versus log (v) plots of the redox peaks located in CV curves in (b).
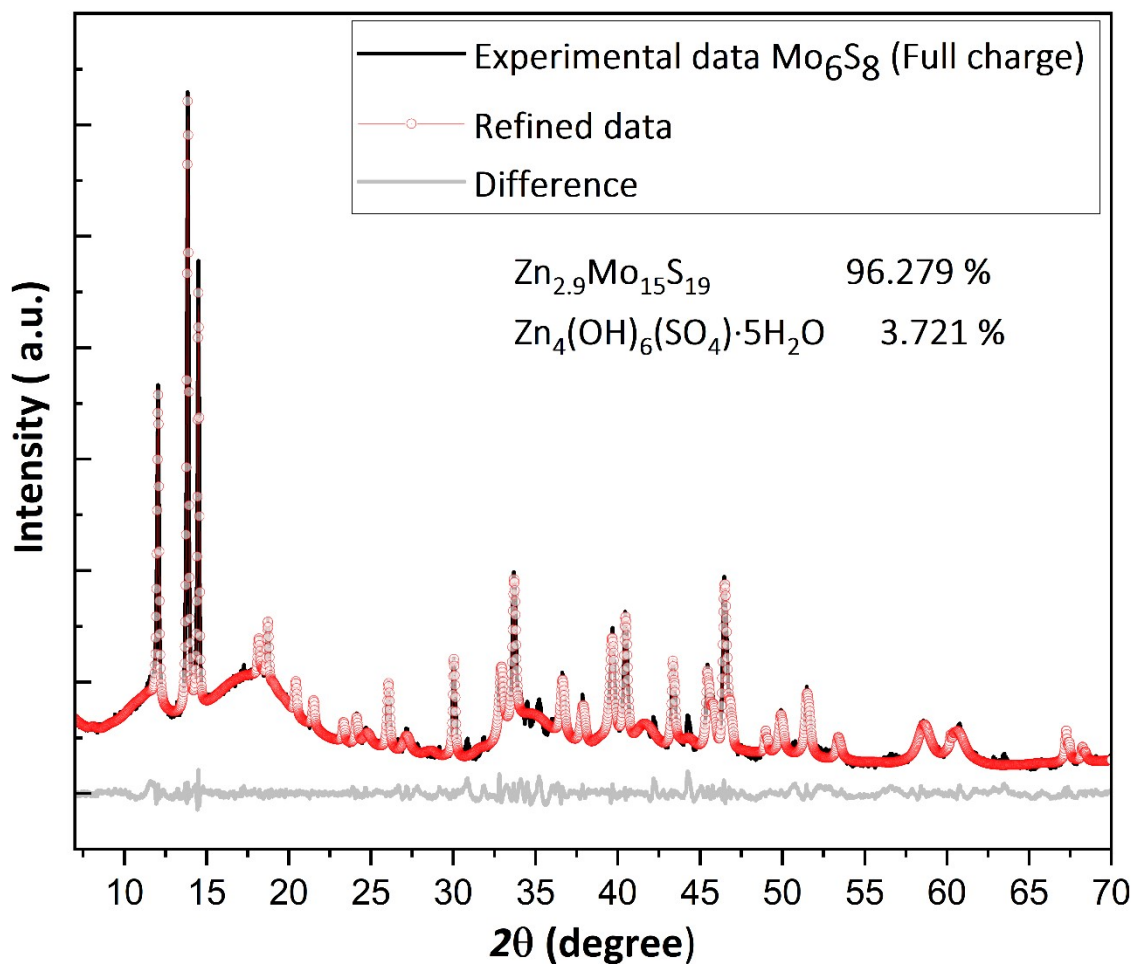
Figure S7. Rietveld XRD refinement fit generated by Topas software of fully charged Mo_6S_8. Data fitted to the standard ICSD used in the XRD phase identifications. (Black line experimental data, red line–refined data, and gray line–difference map between observed and calculated data(residual)). Weighted profile residual: 6.73 and Goodness-of-fit : 2.24

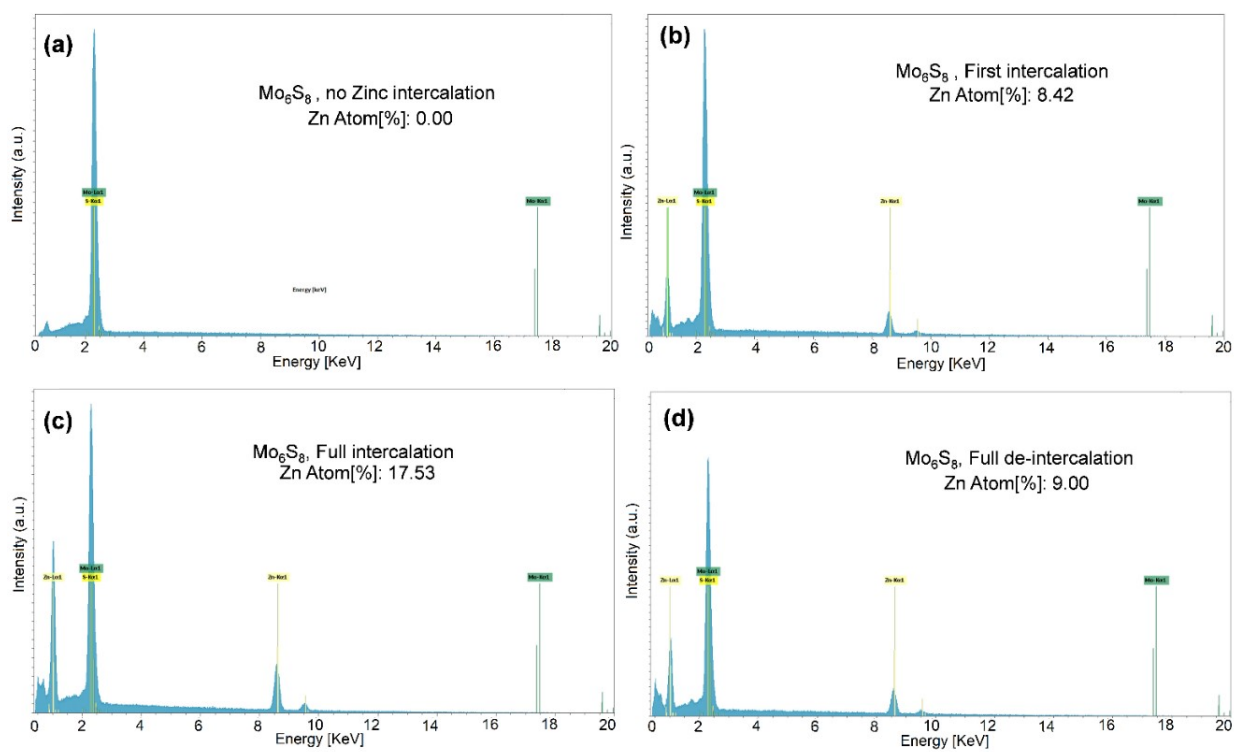**Figure S8.** EDX survey spectra of Zn-intercalated Mo_6S_8 at different state of charge. (a) blank Mo_6S_8 sample at OCP potential. (b) Mo_6S_8 electrode at ~0.5 V vs Zn^{2+}/Zn, (c) at ~0.3 V vs vs Zn^{2+}/Zn, and (d) at 1.0 V vs Zn^{2+}/Zn.
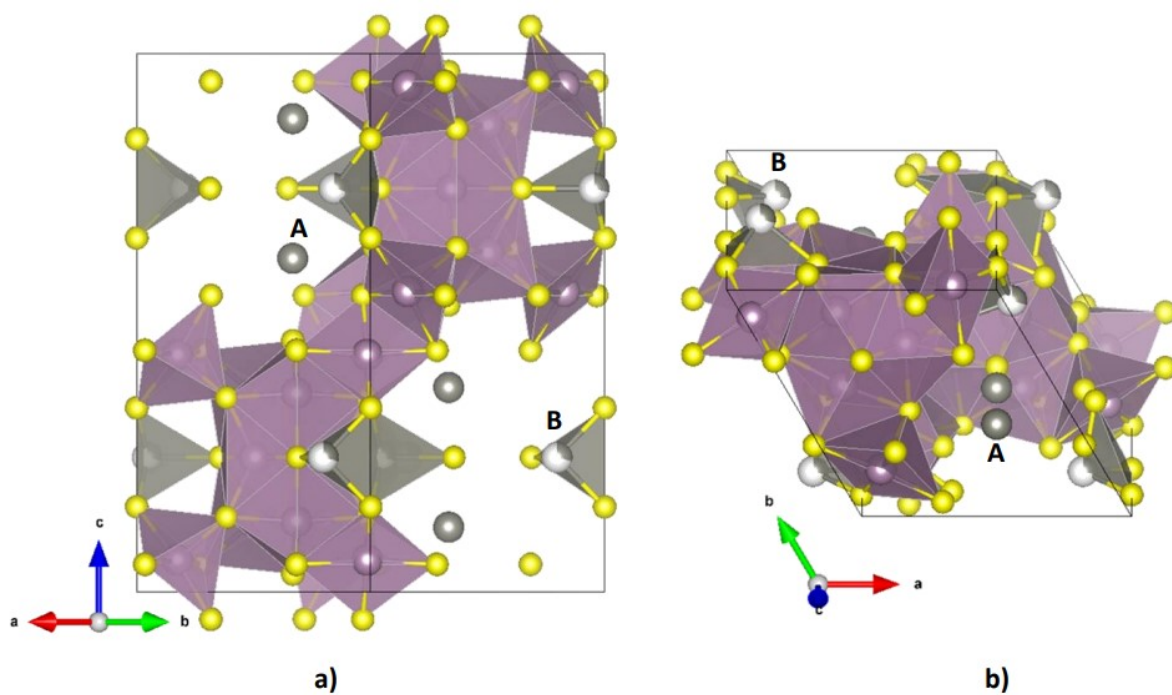
Figure S9. Visual representation of the $Zn_{2.9}Mo_{15}S_{19}$ structure. The Zn atoms are shown in grey, marked A are the 100% occupied sites , the 30% occupation Zn atoms are marked B. Mo is shown in purple and sulfur in yellow. a) shows the side view and b) a slanted top view.
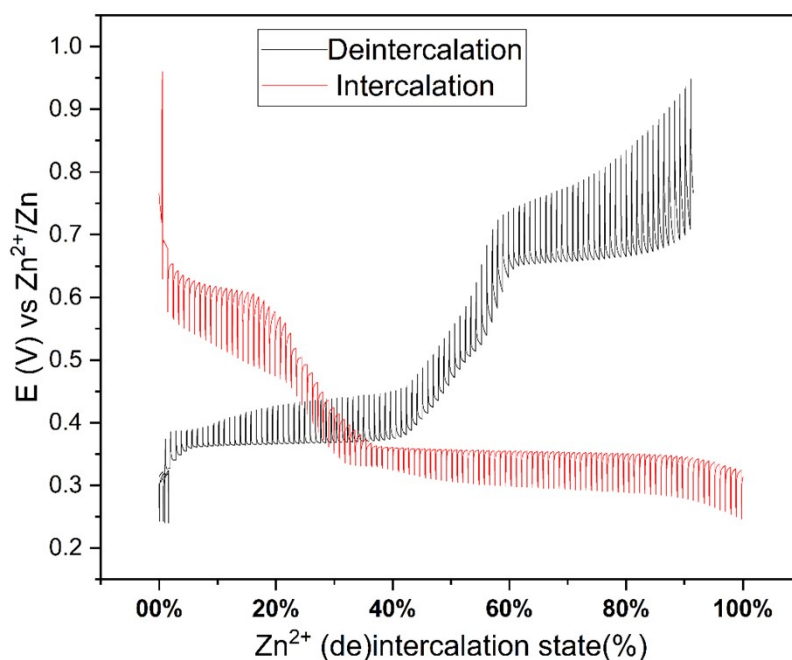
Figure S10. Galvanostatic intermittent titration technique (GITT) curves of in 2M ZnSO$_4$ at 0.1 A/g recorded during the Zn^{2+} intercalation/de-intercalation process.

Table S1. Calculated diffusion coefficient values during the Zn^{2+} intercalation/deintercalation into Mo$_6$S$_8$ process using the GITT technique.

| E(V) vs Zn^{2+}/Zn	D/ cm^2 s^{-1} (intercalation)	log (D(cm^2 s^{-1})) (intercalation)	E(V) vs Zn^{2+}/Zn	D/ cm^2 s^{-1} (de-intercalation)	log (D(cm^2 s^{-1})) (de-intercalation)
0.653	7.90 × 10^{-8}	−7.103	0.328	1.92 × 10^{-7}	−6.716
0.630	1.68 × 10^{-8}	−7.774	0.340	2.66 × 10^{-7}	−6.575
0.576	2.07 × 10^{-8}	−7.683	0.379	2.95 × 10^{-8}	−7.531
0.543	4.99 × 10^{-7}	−6.302	0.406	4.37 × 10^{-8}	−7.359
0.518	1.34 × 10^{-7}	−6.873	0.447	7.09 × 10^{-8}	−7.150
0.479	1.00 × 10^{-7}	−6.999	0.505	2.03 × 10^{-8}	−7.693
0.435	9.61 × 10^{-8}	−7.017	0.560	5.72 × 10^{-8}	−7.243
0.406	5.84 × 10^{-10}	−9.233	0.608	9.03 × 10^{-8}	−7.044
0.373	2.76 × 10^{-9}	−8.559	0.676	0.02 × 10^{-8}	−9.828
0.358	6.76 × 10^{-10}	−9.170	0.708	3.02 × 10^{-9}	−8.520
0.323	1.08 × 10^{-10}	−9.968	-		-
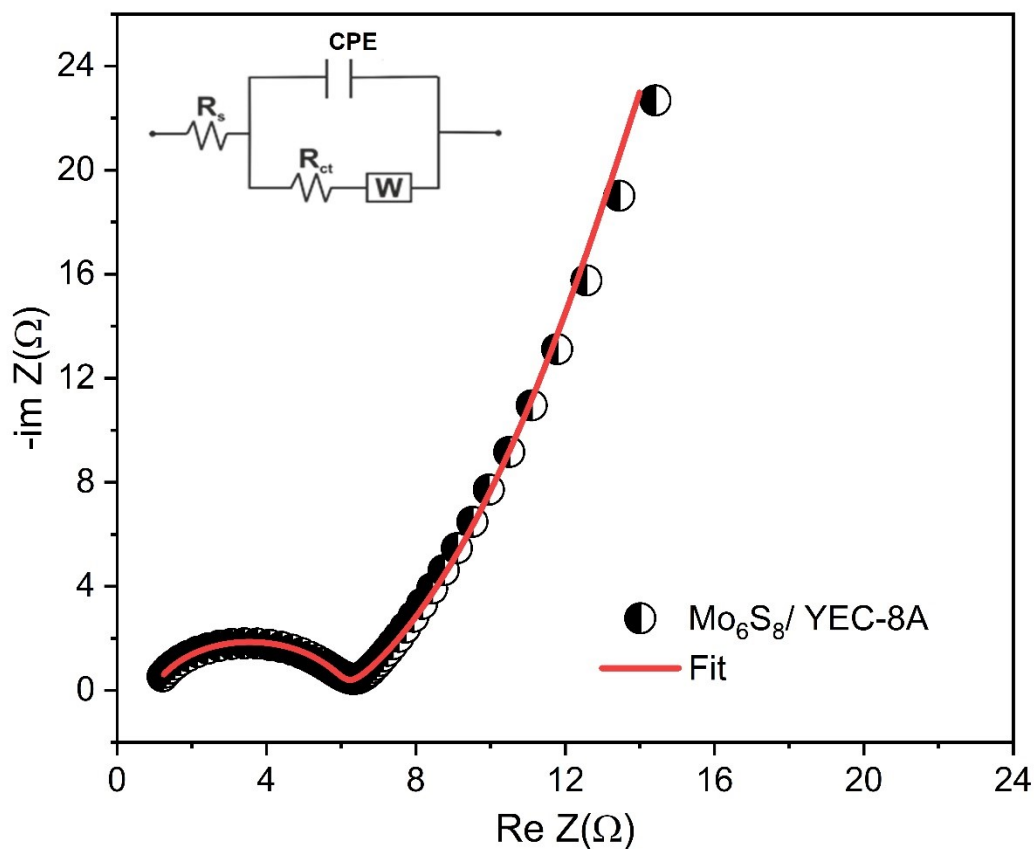
Figure S11. EIS spectrum of the Mo_6S_8/ YEC-8A recorded at the OCP (1.2V) in a frequency range between 0.1Hz and 100.0 kHz with an imposed rms amplitude of 5 mV peak-to-peak.

Table S2. Calculated parameters based on Trasatti analysis including total capacity (Q_{total}), capacity due to surface capacitive contribution ($Q_{capacitive}$), and diffusion contribution capacity ($Q_{diffusion}$)

Electrode	Q_{total} (mAh/g)	$Q_{capacitive}$ (mAh/g)	$\%Q_{capacitive}$ (%)	$Q_{diffusion}$ (mAh/g)	$\%Q_{diffusion}$ (%)
Mo_6S_8	87.64	17.63	20.1	70.01	79.9

- Specific capacitance and energy density calculations.

The specific capacitance for the AC electrode was calculated from the GCD curves as follow.

$$C_{sp} = \frac{I\Delta t}{m\Delta V}$$

where, m is the mass of active material, ΔV represents the voltage range with excluding the IR drop value, I is the discharge current, and t is the discharge time.

The energy (ε) of fabricated Mo_6S_8/AC-YEC was calculated by multiplying the average discharge voltage by its discharge capacity as follow:

$$\varepsilon = \int QVdV$$

The power density is calculated as follow:

$$P = \frac{\varepsilon}{\Delta t}$$

References for SI:

[1]   A. Elgendy, A. A. Papaderakis, C. Byrne, Z. Sun, J. V Lauritsen, E. P. C. Higgins, A. Ejigu, R. Cernik, A. S. Walton, D. J. Lewis, R. A. W. Dryfe, *ACS Appl. Energy Mater.* **2021**, *4*, 13015.

[2]   M. Mao, Z. Lin, Y. Tong, J. Yue, C. Zhao, J. Lu, Q. Zhang, L. Gu, L. Suo, Y.-S. Hu, *ACS Nano* **2019**, *14*, 1102.